PHYSICAL REVIEW B **86**, 094430 (2012)

Full magnetoelectric response of Cr_2O_3 from first principles

Andrei Malashevich,[1,2,*] Sinisa Coh,[1,2] Ivo Souza,[3,4] and David Vanderbilt[5]
[1]*Department of Physics, University of California, Berkeley, California 94720, USA*
[2]*Materials Sciences Division, Lawrence Berkeley National Laboratory, Berkeley, California 94720, USA*
[3]*Centro de Física de Materiales (CSIC) and DIPC, Universidad del País Vasco, 20018 San Sebastián, Spain*
[4]*Ikerbasque Foundation, 48011 Bilbao, Spain*
[5]*Department of Physics and Astronomy, Rutgers University, Piscataway, New Jersey 08854, USA*
(Received 24 July 2012; published 24 September 2012; publisher error corrected 11 April 2013)

The linear magnetoelectric response of Cr_2O_3 at zero temperature is calculated from first principles by tracking the change in magnetization under a macroscopic electric field. Both the spin and the orbital contributions to the induced magnetization are computed, and in each case the response is decomposed into lattice and electronic parts. We find that the transverse response is dominated by the spin-lattice and spin-electronic contributions, whose calculated values are consistent with static and optical magnetoelectric measurements. In the case of the longitudinal response, orbital contributions dominate over spin contributions, but the net calculated longitudinal response remains much smaller than the experimentally measured one at low temperatures. We also discuss the absolute sign of the magnetoelectric coupling in the two time-reversed magnetic domains of Cr_2O_3.

DOI: 10.1103/PhysRevB.86.094430 PACS number(s): 75.85.+t, 75.30.Cr, 71.15.Rf, 71.15.Mb

I. INTRODUCTION

There has been a recent resurgence of interest in magnetoelectric (ME) couplings in solids.[1] Of particular importance is the *linear ME effect*, which can occur in insulating materials with broken inversion and time-reversal symmetries. It can be described by a response tensor:

$$\alpha_{ij}^{\mathcal{E}H} = \left(\frac{\partial P_i}{\partial H_j}\right)_{\boldsymbol{\mathcal{E}}} = \mu_0 \left(\frac{\partial M_j}{\partial \mathcal{E}_i}\right)_{\mathbf{H}}, \tag{1}$$

where $\mathbf{P}$ is the electric polarization induced by the magnetic field $\mathbf{H}$, and conversely $\mathbf{M}$ is the magnetization induced by the electric field $\boldsymbol{\mathcal{E}}$.

The early milestones in the long history of the linear ME effect include the original prediction by Dzyaloshinskii that it should occur in Cr_2O_3[2] and its observation shortly after, both in $\mathbf{M}(\boldsymbol{\mathcal{E}})$[3,4] and in $\mathbf{P}(\mathbf{H})$[5,6] measurements. The ME effect has since been observed in a large variety of materials, but Cr_2O_3 remains one of the best-studied ME compounds. The early literature is surveyed in the monograph by O'Dell,[7] and recent reviews are given in Refs. 1 and 8–10.

Most of the early theoretical work was phenomenological in character, making it difficult to assess the dominant mechanisms behind the ME response. These can be divided into electronic (i.e., frozen-ion) vs lattice responses on the one hand[11] and spin vs orbital magnetic contributions on the other.[12] *Ab initio* theory is an ideal tool for unraveling the microscopic mechanisms of the ME effect in real materials, and the first calculations started to appear in recent years. The initial focus was on spin-lattice contributions,[13,14] in part because investigations of related phenomena in multiferroic materials over the last decade had indicated that spin-lattice effects are often dominant there.[15] In reality, however, very little is known about the relative magnitudes of the various contributions to the ME tensor in typical magnetoelectric materials.

Evidence for a significant electronic ME response in Cr_2O_3 came from optical measurements at frequencies above the lattice resonances: in a series of milestone experiments,[16–18] Pisarev, Krichevtsov, and collaborators observed optical effects governed by an effective ME tensor $\boldsymbol{\alpha}(\omega)$, and found it to be comparable to the static ME coupling. Regarding the distinction between spin and orbital couplings (e.g., how much of the $\boldsymbol{\mathcal{E}}$-field induced magnetization comes from spin moments versus orbital currents), it is probably rather difficult to separate them experimentally due to the weakness of the ME effect in known ME materials. Investigation of the orbital contribution to the ME response is however interesting in its own right. In particular, it was recently established that $\mathbb{Z}_2$ topological insulators with broken time-reversal symmetry on the surface should display a quantized electronic orbital ME response[19,20] with a relatively large quantum ($\alpha = 24.3$ ps/m in SI units). This result further suggests that large orbital ME responses can in principle be achieved even in generic (nontopological) insulators with strong spin-orbit coupling without any constraint on surface preparation.[21]

In this paper, we carry out a thorough first-principles investigation of the linear ME effect in the paradigmatic system Cr_2O_3. We compute the full static response, including on the same footing all four basic contributions: spin-lattice, spin-electronic, orbital-lattice, and orbital-electronic. This completes the program initiated in Refs. 13 and 22, where some but not all of them were evaluated. As in those works, we shall focus exclusively on the ME response at zero temperature, which is determined by mechanisms involving the spin-orbit interaction.

We find that for the response transverse to the rhombohedral axis the spin contributions are much larger than the orbital ones. The calculated values of the lattice and electronic responses are in good agreement with both static and optical ME measurements, as well as with previous calculations. In the case of the longitudinal response the calculated orbital contributions are larger than their spin counterparts in both the electronic and lattice channels. However, as a result of a near cancellation between the orbital-electronic and orbital-lattice contributions, the total calculated longitudinal response is negligibly small. Thus, the nonzero longitudinal response that

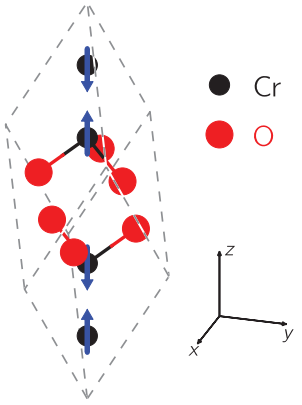

FIG. 1. (Color online) Rhombohedral primitive cell of Cr_2O_3. The arrows indicate the orientations of the *magnetic moments* on the Cr ions (the *spins* on the ions point opposite to the arrows). The center of the cell is a center of inversion symmetry coupled with time reversal.

is measured at low temperatures remains unaccounted for. Some possible reasons for this disagreement will be discussed.

II. PRELIMINARIES

A. Structure of Cr_2O_3

Chromium (III) oxide (eskolaite) crystallizes in a corundum-type structure shown in Fig. 1, with two formula units per primitive cell. The magnetic space group is $R\bar{3}c1'$ above $T_N = 307$ K. Below this temperature Cr_2O_3 turns into an antiferromagnetic (AFM) insulator, with magnetic space group $R\bar{3}'c'$. The magnetic moments on the Cr ions align along the rhombohedral z axis, pointing up and down in an alternating manner (see Fig. 1). The magnetic point group is $\bar{3}'m'$, which allows for a diagonal ME tensor $\boldsymbol{\alpha}$ with two independent components, $\alpha_\perp \equiv \alpha_{xx} = \alpha_{yy}$ (transverse) and $\alpha_\parallel \equiv \alpha_{zz}$ (longitudinal).[23]

We note that there are two distinct possibilities for arranging the magnetic moments in the AFM ground state, related to one another either by time reversal (i.e., by flipping the magnetic moments on every Cr ion) or by spatial inversion. As each of these operations also flips the sign of $\boldsymbol{\alpha}$, it is important to specify which configuration is assumed when reporting values for $\alpha_\perp$ and $\alpha_\parallel$. Our calculations refer to the configuration shown in Fig. 1.

B. Formalism and review of previous calculations

We begin by clarifying issues of units and conventions. Equation (1), which is written in the $(\mathcal{E}, H)$ frame, conforms with the standard experimental definition of the linear ME tensor, which has units of ps/m in SI units. Instead, from the point of view of first-principles theory it is more convenient to work in the $(\mathcal{E}, B)$ frame, where $\boldsymbol{\alpha}$ has units of vacuum admittance $\sqrt{\epsilon_0/\mu_0}$:

$$\alpha_{ij} = \left(\frac{\partial P_i}{\partial B_j}\right)_{\boldsymbol{\mathcal{E}}} = \left(\frac{\partial M_j}{\partial \mathcal{E}_i}\right)_{\mathbf{B}}. \tag{2}$$

The two definitions Eqs. (1) and (2) are related by $\boldsymbol{\alpha}^{\mathcal{E}H} = \mu\boldsymbol{\alpha}$, where μ is the magnetic permeability. In the approximation that $\mu/\mu_0 \simeq 1$, which is a good approximation for most nonferromagnetic materials, the conversion is trivial, and we shall report the calculated values of $\boldsymbol{\alpha}$ as though we had computed them in the $(\mathcal{E}, H)$ frame. For a more detailed discussion, see Sec. II A of Ref. 21.

Let us now discuss how to compute the various contributions to the ME tensor. To recap, the full response can be decomposed into spin and orbital parts according to the nature of the induced magnetization in the $\mathbf{M}(\boldsymbol{\mathcal{E}})$ picture. Each of these can be further decomposed according to the two basic mechanisms by which the field acts on the system. The electronic part describes the ME response that the system would have if the ions were held fixed in their equilibrium positions. The remaining lattice part is associated with the field-induced ionic displacements.

1. Lattice response

We consider first the calculation of lattice couplings. Here the influence of the applied field ($\mathbf{B}$ or $\boldsymbol{\mathcal{E}}$) on the nonconjugate moment ($\mathbf{P}$ or $\mathbf{M}$) is mediated by internal ionic displacements $\mathbf{u}$, so that

$$\boldsymbol{\alpha}^{\text{latt}} = \frac{\partial \mathbf{P}}{\partial \mathbf{u}}\frac{\partial \mathbf{u}}{\partial \mathbf{B}} = \left(\frac{\partial \mathbf{M}}{\partial \mathbf{u}}\frac{\partial \mathbf{u}}{\partial \boldsymbol{\mathcal{E}}}\right)^{\mathrm{T}}, \tag{3}$$

where a summation over the atoms in one crystal cell is implied, and "T" denotes the matrix transpose. (In general there may also be a strain mediated coupling,[14] but in Cr_2O_3 this contribution vanishes by symmetry, and it will not be considered further here.) Optionally, one may also take advantage of the fact that the displacements induced by the field are mediated by field-induced forces $\mathbf{F}$. For the case of applied electric field, Eq. (3) can be rewritten as[13]

$$(\boldsymbol{\alpha}^{\text{latt}})^{\mathrm{T}} = \frac{\partial \mathbf{M}}{\partial \mathbf{u}}\frac{\partial \mathbf{u}}{\partial \mathbf{F}}\frac{\partial \mathbf{F}}{\partial \boldsymbol{\mathcal{E}}} = -\Omega\frac{\partial \mathbf{M}}{\partial \mathbf{u}}\left(\frac{\partial^2 E}{\partial \mathbf{u}\partial \mathbf{u}}\right)^{-1}\left(\frac{\partial \mathbf{P}}{\partial \mathbf{u}}\right)^{\mathrm{T}}, \tag{4}$$

where E is the total energy per unit cell and Ω is the unit-cell volume. Here we have made use of the fact that the Born effective charge tensor can be expressed equivalently as $(\partial \mathbf{F}/\partial \boldsymbol{\mathcal{E}})^{\mathrm{T}} = \Omega\partial \mathbf{P}/\partial \mathbf{u}$. [Alternatively, by invoking the magnetic analog $(\partial \mathbf{F}/\partial \mathbf{B})^{\mathrm{T}} = \Omega\partial \mathbf{M}/\partial \mathbf{u}$ we can arrive at this same equation in a different way, starting from Eq. (3) for the case of applied magnetic induction.] Note that the inverse of the force-constant matrix now appears symmetrically between the magnetic and electric Born tensors in Eq. (4).

There are several choices on how to proceed. One possibility, following Eq. (3), is to relax the structure in the presence of a small $\mathbf{B}$ or $\boldsymbol{\mathcal{E}}$ field, and then compute the relaxation-induced change in $\mathbf{P}$ or $\mathbf{M}$. Alternatively, Eq. (4) expresses $\boldsymbol{\alpha}^{\text{latt}}$ in terms of three basic quantities (the force-constant matrix, the Born charges, and their magnetic analogs), all of which can be computed as changes of various quantities in response to atomic displacements at vanishing fields. One can choose to compute such derivatives by finite differences or by using linear-response techniques available in most density-functional packages.

2. Electronic response

The calculation of the electronic response $\boldsymbol{\alpha}^{\text{el}}$ requires coupling the field $\mathbf{B}$ or $\boldsymbol{\mathcal{E}}$ in Eq. (2) directly to the electrons,

and determining the induced **P** or **M**. In practice this can be done using either finite-field approaches or linear-response techniques.

Of the two contributions, spin-electronic and orbital-electronic, the latter is the most challenging one to calculate. A perturbative expression valid for periodic crystals was recently derived,[24,25] which can be implemented in the context of density-functional perturbation theory. In the present work we have opted to calculate the orbital-electronic response as $\partial \mathbf{M}^{\rm orb}/\partial \boldsymbol{\mathcal{E}}$, using finite electric fields. Another possibility would be to calculate it as $\partial \mathbf{P}/\partial \mathbf{B}^{\rm orb}$, using a finite orbital magnetic field. The inclusion of orbital magnetic fields in total-energy calculations of periodic solids is, however, a challenging problem which has not yet been fully solved, in spite of some recent progress.[25–27]

3. *Review of previous calculations for Cr_2O_3*

The methods described above were recently used to evaluate the spin-lattice and spin-electronic parts of $\boldsymbol{\alpha}$. For the spin-lattice contribution, Íñiguez[13] performed his pioneering calculations following Eq. (4), while Bousquet *et al.*[22] used Eq. (3). More precisely, the latter authors performed structural relaxations in the presence of a fixed Zeeman magnetic field $\mathbf{B}^{\rm spin}$ by adding to the Kohn-Sham energy functional a Zeeman term describing the coupling to the spins. Furthermore, by monitoring the linear change in the electronic polarization $\mathbf{P}^{\rm el}$ under a small field with fixed ions, Bousquet *et al.* were also able to determine the spin-electronic response. Thus, out of the four possible contributions to $\boldsymbol{\alpha}$, only the two spin contributions (lattice and electronic) have previously been evaluated from first principles for Cr_2O_3.

C. Computational approach

Let us now describe the method that we use for calculating the lattice and electronic ME responses, including in each case both the spin and the orbital parts of the response.

For the lattice couplings we employ a method similar to that of Ref. 13 but including also the orbital contribution to $\partial \mathbf{M}/\partial \mathbf{u}$ (we found this to be a more efficient approach than relaxing the lattice under a finite electric field). We first compute the Born effective charges and force-constant matrix using linear-response techniques,[28] and from these we find the first-order field-induced displacements $\Delta \mathbf{u} = (\partial \mathbf{u}/\partial \boldsymbol{\mathcal{E}}) \cdot \Delta \boldsymbol{\mathcal{E}}$, where a nominal field $\Delta \boldsymbol{\mathcal{E}}$ of $\sim 10^9$ V/m is applied along the rhombohedral axis or in the perpendicular direction. Displacing the atoms by $\Delta \mathbf{u}$, we then determine the induced magnetization $\Delta \mathbf{M}^{\rm spin} + \Delta \mathbf{M}^{\rm orb}$. The linearity of the magnetization response was checked by both reducing the magnitude and flipping the sign of $\Delta \boldsymbol{\mathcal{E}}$.

In order to reduce the computational cost, the spin-orbit interaction is not included in the linear-response calculations. This procedure captures the dominant contributions to $\boldsymbol{\alpha}^{\rm latt}$, i.e., those that are linear in the spin-orbit coupling strength; we have checked that it produces results which are almost identical to a calculation in which the spin-orbit coupling is included at every step.

For a given set of ionic displacements $\Delta \mathbf{u}$, the orbital magnetization at $\boldsymbol{\mathcal{E}} = 0$ is calculated under periodic boundary conditions as

$$\mathbf{M}^{\rm orb} = \widetilde{\mathbf{M}}^{\rm LC} + \widetilde{\mathbf{M}}^{\rm IC}, \tag{5}$$

where[29–31]

$$\widetilde{\mathbf{M}}^{\rm LC} = \frac{e}{2\hbar} \int \frac{d^3k}{(2\pi)^3} \mathrm{Im}\, \langle \widetilde{\nabla}_{\mathbf{k}} u_{n\mathbf{k}}| \times H_{\mathbf{k}} |\widetilde{\nabla}_{\mathbf{k}} u_{n\mathbf{k}}\rangle, \tag{6}$$

$$\widetilde{\mathbf{M}}^{\rm IC} = \frac{e}{2\hbar} \int \frac{d^3k}{(2\pi)^3} \mathrm{Im}[\langle u_{n\mathbf{k}}|H_{\mathbf{k}}|u_{m\mathbf{k}}\rangle \times \langle \widetilde{\nabla}_{\mathbf{k}} u_{m\mathbf{k}}| \times |\widetilde{\nabla}_{\mathbf{k}} u_{n\mathbf{k}}\rangle]. \tag{7}$$

Here LC and IC stand for *local circulation* and *itinerant circulation*, respectively, $|u_{n\mathbf{k}}\rangle$ is the cell-periodic part of the Bloch state $|\psi_{n\mathbf{k}}\rangle$, and $H_{\mathbf{k}} = e^{-i\mathbf{k}\cdot\mathbf{r}} \mathcal{H} e^{i\mathbf{k}\cdot\mathbf{r}}$, where $\mathcal{H}$ is the Kohn-Sham Hamiltonian of the crystal. Summations over occupied bands are implied for repeated band indices, and $\widetilde{\nabla}_{\mathbf{k}} \equiv (1 - |u_{n\mathbf{k}}\rangle\langle u_{n\mathbf{k}}|)\nabla_{\mathbf{k}}$. In practice the Brillouin-zone integral is replaced by a summation over a uniform grid, and $\widetilde{\nabla}_{\mathbf{k}}$ is evaluated on that grid by finite differences.[31] $\widetilde{\mathbf{M}}^{\rm LC}$ and $\widetilde{\mathbf{M}}^{\rm IC}$ are separately gauge-invariant, i.e., they remain unchanged under k-dependent unitary transformations among the occupied states.

Let us now turn to the electronic response, which we calculate as $\partial \mathbf{M}/\partial \boldsymbol{\mathcal{E}}$, taking advantage of the well-established *ab initio* treatment of homogeneous electric fields in periodic insulators.[32] The magnetization $\mathbf{M}^{\rm spin} + \mathbf{M}^{\rm orb}$ is determined with and without an electric field of intensity $\sim 10^9$ V/m (using in both cases the same crystal structure optimized at zero field) in order to extract the spin-electronic and orbital-electronic ME couplings. The evaluation of spin magnetization is straightforward and here we just mention that, as an additional check, we have recomputed the spin-electronic coupling using the converse Zeeman-field approach, finding good agreement between the two methods.

To compute $\mathbf{M}^{\rm orb}$ at finite $\boldsymbol{\mathcal{E}}$, we make use of the following generalization of Eqs. (5)–(7).[24] One part is given by the same expression valid at zero field, Eqs. (6) and (7), upon reinterpreting the states $|u_{n\mathbf{k}}\rangle$ therein as field-polarized Bloch states[32] (and $\mathcal{H}$ as the crystal Hamiltonian calculated from the field-polarized periodic charge density). To this, an additional contribution of the form

$$\mathbf{M}^{\rm CS} = -\frac{e^2}{2\hbar} \boldsymbol{\mathcal{E}} \int \frac{d^3k}{(2\pi)^3} \mathrm{Tr} \left[\mathbf{A} \cdot \nabla_{\mathbf{k}} \times \mathbf{A} - \frac{2i}{3} \mathbf{A} \cdot \mathbf{A} \times \mathbf{A} \right] \tag{8}$$

must be added in order to obtain the full orbital magnetization. Here $\mathbf{A}^{nm}_{\mathbf{k}} \equiv i \langle u_{n\mathbf{k}}| \nabla_{\mathbf{k}} |u_{n\mathbf{k}}\rangle$ is the Berry connection matrix; the integrand is a scalar known as the Chern-Simons 3-form[19,20] (band indices are suppressed). Thus, at $\boldsymbol{\mathcal{E}} \neq 0$ we have, instead of Eq. (5),

$$\mathbf{M}^{\rm orb} = \widetilde{\mathbf{M}}^{\rm LC} + \widetilde{\mathbf{M}}^{\rm IC} + \mathbf{M}^{\rm CS}, \tag{9}$$

and all three terms contribute to the orbital-electronic ME response. The term $\boldsymbol{\alpha}^{\rm CS}$ is purely isotropic and can be calculated from the valence Bloch states at zero field. Its numerical evaluation requires a smooth gauge in k space, and this can be achieved by mapping the valence bands onto localized Wannier functions.[21]

D. Technical details

The total-energy and linear-response calculations were performed using the QUANTUM-ESPRESSO[33] *ab initio* code package, working in a fully relativistic framework where the spin-orbit interaction is included in the atomic pseudopotentials. We employed Troullier-Martins norm-conserving pseudopotentials,[34] which in the case of Cr included the semicore $3s$ and $3p$ states in the valence.

The wave functions in the solid were expanded in plane waves with an energy cutoff of 250 Ry for structural relaxations and linear-response calculations and 150 Ry for orbital magnetization calculations. The Brillouin zone was sampled on a $4 \times 4 \times 4$ Monkhorst-Pack mesh for most self-consistent-field (SCF) calculations. While this mesh density produced converged values for the spin-lattice and spin-electronic ME contributions, the two orbital contributions converged more slowly with k-point sampling [this is probably related to the finite-differences representation of the covariant derivatives in Eqs. (6) and (7)]. After testing several grid densities, we concluded that a $7 \times 7 \times 7$ mesh gave sufficiently converged values.

As noted in Ref. 13, the computation of ME couplings demands a very tight tolerance on the convergence of the self-consistent field loop. We therefore used rather stringent convergence thresholds, of the order of 10^{-11}–10^{-12} Ry in the total energy. In order to reach this level of convergence in a reasonable number of steps with QUANTUM-ESPRESSO, we found it useful to use the Thomas-Fermi charge mixing scheme,[36] by setting the input variable "mixing mode" to "local-TF." We also found that the speed of convergence of the calculations with a finite electric field was improved by increasing the field gradually from zero in small steps.

The exchange-correlation potential was described within the generalized-gradient approximation (GGA) using the Perdew-Burke-Ernzerhof (PBE) parametrization.[37] This choice was made after having optimized the structure using both the local-density approximation (LDA) and PBE, and finding that the latter produced structural parameters in better agreement with experiment (see Table I). In particular, LDA underestimates the unit-cell volume by 7.3% while PBE overestimates it by only 1.7%. We note that the authors of Refs. 13 and 22 used LDA + U with the experimental cell volume enforced. As for the magnetic structure, the staggered spin moments on the Cr atoms have a value of 2.7 μ_B/atom, for a sphere integration radius of 1.3 Å. This is in good agreement with the LDA + U value reported in Ref. 13.

TABLE I. Calculated and experimental structural parameters of Cr_2O_3 in the antiferromagnetic phase: rhombohedral lattice parameter a, rhombohedral angle α, and Wyckoff positions of the Cr ions ($4c$ orbit) and O ions ($6e$ orbit).

			Wyckoff positions	
	a (Å)	α (deg)	Cr	O
PBE (this work)	5.415	54.45	0.1541	0.0597
LDA (Ref. 21)	5.322	53.01	0.1575	0.0690
Expt. (Ref. 35)	5.358	55.0	0.1528	0.0566

TABLE II. Calculated contributions to the magnetoelectric tensor components $\alpha_\perp$ and $\alpha_\parallel$ in Cr_2O_3. Columns (rows) show the spin and orbital (electronic and lattice) contributions. (The results from previous calculations are indicated in parentheses.)

	$\alpha_\perp$ (ps/m)			$\alpha_\parallel$ (ps/m)		
	Spin	Orb.	Total	Spin	Orb.	Total
Elec.	0.26 (0.34[a])	−0.014	0.25	0.0007 (0[a])	−0.009	−0.008
Latt.	0.77 (1.11[a]) (0.43[b])	0.025	0.80	0.0026 (0[a]) (0.00[b])	0.008	0.011
Total	1.03	0.011	1.04	0.003	−0.001	0.002

[a]Reference 22.
[b]Reference 13.

III. RESULTS

A. Contributions to the ME response

The main results of our calculations are presented in Table II together with results from previous theoretical works, given in parentheses. Let us first analyze the transverse ME response. The magnitude of the calculated static value, $|\alpha_\perp| = 1.04$ ps/m, agrees well with the most reliable measurements, which range from 0.7 to 1.6 ps/m.[38,39] The spin-lattice contribution accounts for about 75% of that value, with the remaining 25% coming mostly from the spin-electronic response, while the two orbital contributions are negligible (less than 2%). The values we obtain for the individual contributions $\alpha_\perp^{\text{latt}}$ and $\alpha_\perp^{\text{el}}$ agree well with those calculated in Ref. 22 using the converse Zeeman-field approach.

In the case of the longitudinal response, the relative strengths of the four contributions are very different. As in previous calculations,[13,22] we find that the spin contributions to $\alpha_\parallel$ are very small, summing to only 0.003 ps/m in our calculation. This can be understood as resulting from the extreme stiffness of the magnitude of the spin moment in a collinear band antiferromagnet, which is also reflected in the near-vanishing of the spin magnetic susceptibility $\chi_\parallel$ at $T = 0$.[12]

Experimentally, however, the low-temperature $\alpha_\parallel$ is found to be about 0.2–0.3 ps/m.[38,39] This is smaller than $\alpha_\perp$ by a factor of 3 to 6, but still about two orders of magnitude larger than our theoretical spin value, suggesting that orbital effects might be responsible for most of the $\alpha_\parallel$ response. Indeed, Hornreich and Shtrikman[12] pointed out that a zero-temperature longitudinal ME response could arise in Cr_2O_3 from an electric-field-induced shift in the g factor of the Cr ions (see also Ref. 11). This is an orbital effect that should be automatically included in the present calculations. In fact, we do find that our computed orbital-lattice and orbital-electronic contributions to $\alpha_\parallel$ are nearly an order of magnitude larger than the corresponding spin contributions. However, the orbital-lattice and orbital-electronic contributions individually are still an order of magnitude smaller than the measured value. Moreover, these two contributions have opposite signs, resulting in a near cancellation of the entire longitudinal response. Our total $\alpha_\parallel$ of 0.002 ps/m thus remains about two orders of magnitude smaller than the measured value.

TABLE III. Decomposition of the calculated orbital ME response of Cr_2O_3 (presented in Table II) into "local circulation," "itinerant circulation," and "Chern-Simons" contributions coming respectively from Eqs. (6), (7), and (8).

$\boldsymbol{\alpha}^{\mathrm{orb}}$ (ps/m)	$\alpha_{\perp}^{\mathrm{orb}}$	$\alpha_{\parallel}^{\mathrm{orb}}$
Electronic		
Local circulation	−0.0064	−0.0237
Itinerant circulation	−0.0084	0.0135
Chern-Simons	0.0012	0.0012
Subtotal	−0.0136	−0.0090
Lattice		
Local circulation	0.0202	0.0078
Itinerant circulation	0.0051	0.0000
Subtotal	0.0253	0.0078
Total	0.0117	−0.0012

There are several possible explanations for this discrepancy. First, the theoretical values for the orbital longitudinal response are quite small, and thus might be especially sensitive to numerical errors. However, we have checked k-point and self-consistent convergence carefully, and do not believe this is a major concern. More serious is the potential dependence on choice of exchange-correlation potential. In particular, within the LDA we found that the orbital-electronic and orbital-lattice contributions are approximately a factor of 3 larger compared to PBE, although similar cancellation of the two contributions was observed. Future work is needed to check the sensitivity of these calculations to the choice of GGA (adopted here) as opposed to LDA, LDA + U or GGA + U, hybrid functionals, or other orbital-dependent functionals. Since orbital currents play a crucial role, the use of current-density functionals should probably also be explored. On the experimental side, it would probably be advisable to check the dependence of the measured value on sample quality, in order to rule out extrinsic effects associated with defects, surfaces, contacts, etc.

It is also possible, however, that the experimentally observed response is dominated by some physics not captured by LDA or GGA approximations to the exact density functional. For example, the strong dependence of $\alpha_{\parallel}$ upon temperature makes it clear that thermal fluctuations strongly influence the longitudinal response. By the same token, it is possible that quantum spin fluctuations, already present in the antiferromagnetic state at zero temperature, may play an important role. For the time being, we leave this as an open question.

Before closing this section, we recall that the orbital ME response can be further decomposed into local circulation (LC), itinerant circulation (IC), and—in the case of the orbital-electronic response—Chern-Simons (CS) contributions, as in Eq. (9). Table III shows the breakdown of the full orbital response computed in the present work. In our previous study of Cr_2O_3, only the isotropic CS term was calculated (using LDA rather than GGA).[21] In that work we found the CS term to be ∼0.01 ps/m, about an order of magnitude larger than the presently calculated value. Further work is needed to determine how the various terms in the ME response of Cr_2O_3 depend on the choice of exchange-correlation potential. It can be seen that the CS contribution to the orbital-electronic response is about an order of magnitude smaller than the LC and IC contributions. Individually, the LC and IC orbital-electronic contributions are somewhat larger for $\alpha_{\parallel}$ than for $\alpha_{\perp}$, but taken together the opposite is true. As for the orbital-lattice contributions to $\alpha_{\perp}$ and $\alpha_{\parallel}$, they come mainly from the LC terms.

B. Sign of the ME response

We now discuss the overall sign of the tensor $\boldsymbol{\alpha}$. As already mentioned, in Cr_2O_3 this sign depends on the orientation of the magnetic moments (see Fig. 1). Experimentally, a single AFM domain can be stabilized by cooling the sample through the Néel temperature in the presence of parallel (or antiparallel) electric and magnetic fields ("magnetoelectric annealing"), and the spin structure can then be analyzed using spherical neutron polarimetry.[40,41]

According to Ref. 40, the orientation of the magnetic moments shown in Fig. 1 therein corresponds to a domain annealed with electric and magnetic fields pointing in the opposite direction along the rhombohedral axis, provided that arrows in that figure indeed indicate directions of spin moments rather than magnetizations. Since the magnetoelectric tensor appears in the free energy in the form $F_{\mathrm{ME}} = -\alpha_{ij}\mathcal{E}_i H_j$, the domain under consideration should have negative $\alpha_{\parallel}$ near the Néel temperature. Experimental measurements of magnetoelectric coupling as a function of temperature[38,39] show that $\alpha_{\parallel}$ changes sign around 100 K, while $\alpha_{\perp}$ is negative all the way to 4.2 K. Assuming that magnetic domain is determined at high temperatures, close to the Néel temperature, and that magnetic domains remain frozen upon cooling to 4.2 K, we can conclude that at 4.2 K the domain shown in Fig. 1 must have $\alpha_{\perp} > 0$ and $\alpha_{\parallel} > 0$.

Our computed signs appear to agree with the experimental work of Ref. 40, although it was not made entirely clear whether the signs reported there refer to spins or magnetizations. Now that first-principles theory is seriously beginning to confront experiment in the field of magnetoelectric couplings, we urge closer attention to sign issues in future investigations, both theoretical and experimental.

C. Comparison to optical measurements

We now turn to the comparison with existing measurements of the optical ME tensor $\boldsymbol{\alpha}(\omega)$. As our theory only deals with static fields, the calculated $\boldsymbol{\alpha}^{\mathrm{el}}$ should be thought of as the $\omega \to 0$ limit of the purely electronic optical response (quasistatic limit). This is expected to approximate reasonably well the measured response at frequencies between the lattice and electronic resonances and sufficiently far from both.

The ME coupling influences both the transmission and reflection of light from a magnetoelectric medium, giving rise to characteristic optical effects which are odd under time reversal.[11,42] While the propagation of electromagnetic waves inside a ME medium is only affected by the traceless part of $\boldsymbol{\alpha}$, all tensor components can in principle be extracted from reflectance measurements, although in that case the net effect may also have surface-specific contributions.[17] The reflection experiments of Ref. 17 were carried out using visible light with a wavelength of 633 nm (1.96 eV), which falls within

the exciton absorption range of Cr_2O_3, thus precluding a meaningful comparison with our quasistatic calculations.

We therefore focus on the earlier transmission measurements,[16] which used near infrared light of 1156 nm (1.07 eV). The effect that was observed consists of a tilt away from the crystallographic $\hat{\mathbf{y}}$ and $\hat{\mathbf{z}}$ directions of the linear polarization of light traveling along $\hat{\mathbf{x}}$. The tilt angle ϕ is related to the components of the optical ME tensor (expressed in Gaussian units) and index of refraction by[17,42]

$$\phi \simeq -\frac{1}{2}\frac{\alpha_{zz}-\alpha_{xx}}{n_z-n_x}. \tag{10}$$

While an effect which changed sign between time-reversed samples was clearly observed, a time-even background signal of comparable magnitude could not be eliminated. The most reliable value, $\phi = 4' \simeq 1.2\times10^{-3}$ rad, was measured at 220–240 K. As the absolute value of the linear birefringence was not reported, we use the value $n_z - n_x = 5.8\times10^{-2}$ quoted in Ref. 17 for 633 nm, to arrive at $\alpha_{xx}-\alpha_{zz}\sim 0.12$ ps/m. The agreement with our calculated value of 0.26 ps/m is quite satisfactory, given the experimental uncertainties as well as the limitations in our theory (namely, the DFT underestimation of the optical gap and the assumed quasistatic and low-temperature limits in the calculation).

We emphasize that, as in the case of the static measurements discussed earlier, the dominant type of AFM domain present in the samples was not specified in Ref. 16. Hence the *absolute* sign of the measured optical ME coefficient was not determined. It would be interesting to carry out optical and static ME measurements on the same single-domain sample at low temperatures. This would allow one to extract the *relative* sign between $\alpha_\perp^{\rm el}$ and $\alpha_\perp^{\rm latt}+\alpha_\perp^{\rm el}$, which we predict to be positive.

IV. CONCLUSIONS

In summary, we have performed a thorough investigation of the zero-temperature ME response in Cr_2O_3 using first-principles calculations. We analyzed the lattice and electronic parts of the response including both spin and orbital magnetization contributions, being careful to treat all four contributions on an equal footing. In particular, we treated the orbital response using the modern Berry-phase theory, without introducing muffin-tin approximations, in which orbital currents are computed inside spheres around atoms.

We have then compared the calculated values with static and optical measurements. Previous calculations, which focused on the spin contributions, had found an essentially null value for $\alpha_\parallel$, in disagreement with experiment. We therefore set out to check whether orbital effects could account for the observed low-temperature longitudinal response, as had been proposed early on in the literature. Our results suggest that this is not the case, as the calculated orbital responses are very small, consistent with a scenario of strongly quenched orbital moments. We hope that the present findings will stimulate further investigations, both on the experimental and theoretical sides.

Recently we became aware of concurrent first-principles studies of the orbital ME response in Cr_2O_3[43] and $LiFePO_4$[44] using the approximation of integrating orbital currents within atom-centered spheres.

ACKNOWLEDGMENTS

This work was supported by NSF Grant No. DMR-10-05838 and by Grant No. MAT2012-33720 from the Spanish Ministerio de Economía y Competitividad. We would like to thank Michael Fechner, Manish Jain, and Georgy Samsonidze for useful discussions.

*andreim@civet.berkeley.edu.

[1] M. Fiebig, J. Phys. D **38**, R123 (2005).
[2] I. E. Dzyaloshinskii, Sov. Phys. JETP **10**, 628 (1960).
[3] D. N. Astrov, Sov. Phys. JETP **11**, 708 (1960).
[4] D. N. Astrov, Sov. Phys. JETP **13**, 729 (1961).
[5] V. J. Folen, G. T. Rado, and E. W. Stalder, Phys. Rev. Lett. **6**, 607 (1961).
[6] G. T. Rado and V. J. Folen, Phys. Rev. Lett. **7**, 310 (1961).
[7] T. H. O'Dell, *The Electrodynamics of Magnetoelectric Media* (North-Holland, Amsterdam, 1970).
[8] W. Eerenstein, N. D. Mathur, and J. F. Scott, Nature (London) **442**, 759 (2006).
[9] M. Fiebig and N. A. Spaldin, Eur. Phys. J. B **71**, 293 (2009).
[10] J.-P. Rivera, Eur. Phys. J. B **71**, 299 (2009).
[11] O. F. de Alcantara Bonfim and G. A. Gehring, Adv. Phys. **29**, 731 (1980).
[12] R. Hornreich and S. Shtrikman, Phys. Rev. **161**, 506 (1967).
[13] J. Íñiguez, Phys. Rev. Lett. **101**, 117201 (2008).
[14] J. C. Wojdeł and J. Íñiguez, Phys. Rev. Lett. **103**, 267205 (2009).
[15] S.-W. Cheong and M. Mostovoy, Nat. Mater. **6**, 13 (2007).
[16] R. V. Pisarev, B. B. Krichevtsov, and V. V. Pavlov, Phase Transitions **37**, 63 (1991).
[17] B. B. Krichevtsov, V. V. Pavlov, R. V. Pisarev, and V. N. Gridnev, J. Phys.: Condens. Matter **5**, 8233 (1993).
[18] B. B. Krichevtsov, V. V. Pavlov, R. V. Pisarev, and V. N. Gridnev, Phys. Rev. Lett. **76**, 4628 (1996).
[19] X.-L. Qi, T. L. Hughes, and S.-C. Zhang, Phys. Rev. B **78**, 195424 (2008).
[20] A. M. Essin, J. E. Moore, and D. Vanderbilt, Phys. Rev. Lett. **102**, 146805 (2009).
[21] S. Coh, D. Vanderbilt, A. Malashevich, and I. Souza, Phys. Rev. B **83**, 085108 (2011).
[22] E. Bousquet, N. A. Spaldin, and K. T. Delaney, Phys. Rev. Lett. **106**, 107202 (2011).
[23] R. E. Newnham, *Properties of Materials* (Oxford University Press, New York, 2005).
[24] A. Malashevich, I. Souza, S. Coh, and D. Vanderbilt, New J. Phys. **12**, 053032 (2010).
[25] A. M. Essin, A. M. Turner, J. E. Moore, and D. Vanderbilt, Phys. Rev. B **81**, 205104 (2010).
[26] W. Cai and G. Galli, Phys. Rev. Lett. **92**, 186402 (2004).

[27]X. Gonze and J. W. Zwanziger, Phys. Rev. B **84**, 064445 (2011).
[28]S. Baroni, S. de Gironcoli, A. D. Corso, and P. Giannozzi, Rev. Mod. Phys. **73**, 515 (2001).
[29]D. Xiao, J. Shi, and Q. Niu, Phys. Rev. Lett. **95**, 137204 (2005).
[30]T. Thonhauser, D. Ceresoli, D. Vanderbilt, and R. Resta, Phys. Rev. Lett. **95**, 137205 (2005).
[31]D. Ceresoli, T. Thonhauser, D. Vanderbilt, and R. Resta, Phys. Rev. B **74**, 024408 (2006).
[32]I. Souza, J. Íñiguez, and D. Vanderbilt, Phys. Rev. Lett. **89**, 117602 (2002).
[33]P. Giannozzi *et al*., J. Phys.: Condens. Matter **21**, 395502 (2009).
[34]N. Troullier and J. L. Martins, Phys. Rev. B **43**, 1993 (1991).
[35]A. H. Hill, A. Harrison, C. Dickinson, W. Zhou, and W. Kockelmann, Microporous Mesoporous Mater. **130**, 280 (2010).
[36]D. Raczkowski, A. Canning, and L. W. Wang, Phys. Rev. B **64**, 121101 (2001).
[37]J. P. Perdew, K. Burke, and M. Ernzerhof, Phys. Rev. Lett. **77**, 3865 (1996).
[38]E. Kita, K. Siratori, and A. Tasaki, J. Appl. Phys. **50**, 7748 (1979).
[39]H. Wiegelmann, A. G. M. Jansen, J.-P. Rivera, and H. Schmid, Ferroelectrics **162**, 141 (1994).
[40]P. J. Brown, J. B. Forsyth, E. Lelievre-Berna, and F. Tasset, J. Phys.: Condens. Matter **14**, 1957 (2002).
[41]P. J. Brown, J. B. Forsyth, and F. Tasset, Solid State Sci. **7**, 682 (2005).
[42]R. M. Hornreich and S. Shtrikman, Phys. Rev. **171**, 1065 (1968).
[43]M. Fechner *et al*. (unpublished).
[44]A. Scaramucci, E. Bousquet, M. Fechner, M. Mostovoy, and N. A. Spaldin, arXiv:1207.2916.